Journal of Solid State Chemistry **146,** 448–457 (1999)
Article ID jssc.1999.8389, available online at http://www.idealibrary.com on IDEAL®

# Oxygen Content and Structures of $La_{1-x}Ca_xMnO_{3+d}$ as a Function of Synthesis Conditions

B. Dabrowski,[1] R. Dybzinski, Z. Bukowski,[2] and O. Chmaissem

*Department of Physics, Northern Illinois University, DeKalb, Illinois 60115*

and

J. D. Jorgensen

*Materials Science Division, Argonne National Laboratory, Argonne, Illinois 60439*

Received March 9, 1999; in revised form April 28, 1999; accepted May 21, 1999

**Using thermogravimetric analysis measurements, oxygen content was measured for $La_{1-x}Ca_xMnO_{3+d}$ ($0 \le x \le 0.38$) samples prepared at high oxygen pressure. The oxygen content was found to decrease uniformly with increasing $x$ for samples annealed at 12 and 140 atm $O_2$ at 800°C, slowly cooled in 1, 20, and 100% $O_2$, as well as for samples in thermal equilibrium at high temperatures of $\sim 1000-1400$°C. Annealing at a specific temperature and oxygen pressure leads to approximately constant hole doping over an extended range of Ca substitution $x$. The most favorable synthesis conditions for obtaining stoichiometric, $d = 0$, samples were determined. The data suggest that several studies reported in the literature were done on significantly nonstoichiometric materials. Structural results show that, in addition to the orthorhombic *Pbnm* O′ ($c/a < \sqrt{2}$) and O* ($a \sim b \sim c/\sqrt{2}$) structures, the rhombohedral $R\bar{3}c$ structure is stabilized at high oxygen contents for $x \le 0.14$. A sequence of observed structures and a decrease of the unit cell volume with increasing $d$ confirm that the additional holes are doped uniformly by cation-vacancy defects for all studied $x$.** © 1999 Academic Press

***Key Words*: colossal magnetoresistance; cation nonstoichiometry; thermogravimetry; structural properties.**

## INTRODUCTION

Pure and substituted $LaMnO_3$ materials have been the subject of intense research owing to their technological importance for use in solid oxide fuel cells, oxygen sensors, catalysts, and more recently, due to the colossal magnetoresistive (CMR) effect observed near the Curie temperature, $T_c$ (1–3). Most of the catalytic, reactive, physical, and structural properties have been directly related to the amount of substituted alkaline earth, the size of the substituted ion, and the variance of the ionic sizes (4–6). Recent studies have also established that the structural, electrical, and magnetic properties are a function of the synthesis conditions that affect the chemical stoichiometry of the compound (7, 8). Considerable deviations from nominal stoichiometry were reported to be caused by the formation of vacancies on the metal sites during synthesis under oxidizing conditions or vacancies on oxygen sites during synthesis under reducing conditions (9–11).

Extensive studies of the cation and oxygen nonstoichiometry have been done for pure $LaMnO_{3+d}$ using wet-chemical redox titration methods on quenched samples, and thermogravimetric measurements (TGA) and coulometric titrations *in situ* (9–15). These studies have found that the ratio of oxygen to metal ion, $3 + d$:1, is a function of temperature and partial pressure of oxygen at high temperatures. Stoichiometric $LaMnO_3$ ($d = 0$) can be synthesized only at low partial pressures of oxygen, for example, the recent work of Topfer and Goodenough (16) cites values of $-8 \le \log P(O_2) \le -5$ at 1200°C and $-12 \le \log P(O_2) \le -7$ at 1000°C. A compilation of earlier experimental data on the relationship between $P(O_2)$ and the composition of $LaMnO_{3+d}$ for $-6 \le \log P(O_2) \le 0$ was given by van Roosmalen and Cordfunke (14, 15). Their data showed, for example, that in pure oxygen $d \sim 0.06$ and 0.10 at 1200 and 1000°C, respectively. Based on an observation that $d$ does not usually exceed 0.2, van Roosmalen and Cordfunke (14, 15) introduced a cation-vacancy defect model that describes the relation between $P(O_2)$ and $d$ in terms of the charge disproportionation of $Mn^{3+}$ into $Mn^{2+}$ and $Mn^{4+}$. Recently, however, larger values of $d$, up to $d = 0.31$, were reported for samples prepared at high oxygen pressures or for samples processed

[1] To whom correspondence should be addressed. E-mail: dabrowski@anl.gov.

[2] Also at Institute of Low Temperature and Structure Research, Polish Academy of Sciences, P.O. Box 937, 50-950 Wroclaw, Poland.



0022-4596/99 $30.00

directly from metal citrates at lower temperatures, 700–1000°C (17, 18).

Using density measurements, structural studies by high-resolution electron microscopy and neutron powder diffraction, and thermodynamic considerations of defect models, it was shown that vacancies on the $A$ and $B$ sites form in approximately equal amounts, i.e., $v \sim v_A \sim v_B \sim d/(3+d)$ (12–14). Thus, there is no oxygen in an additional defect site and the chemical formula for the compound should read $La_{3/(3+d)}Mn_{3/(3+d)}O_3$. For convenience, however, the notation in terms of the "excess" oxygen content $LaMnO_{3+d}$ is usually used, and we will adopt this notation. Samples with unequal amounts of vacancies ($v_{La} \neq v_{Mn}$) can be intentionally or unintentionally obtained resulting in different relations between $d$ and $P(O_2)$ than reported for $LaMnO_{3+d}$ (9, 10, 14, 16, 19, 20). Furthermore, several studies were also done at very low partial pressures of oxygen, $-17 \leq \log P(O_2) \leq -9$, showing that small amounts of oxygen vacancies, $d \sim -0.015$ to $-0.095$, can be obtained between 900 and 1450°C (9–11).

There is little data on the relationship between synthesis conditions and chemical stoichiometry available for substituted $La_{1-x}A_xMnO_3$ materials ($A$ = Ba, Sr, Ca), (8, 13–15, 21–25). Based on TGA measurements for $La_{0.85}Sr_{0.15}MnO_3$ van Roosmalen and Cordfunke (13–15) concluded that the defect chemistry of $La_{1-x}Sr_xMnO_{3+d}$ is based on the same defect formation as for $LaMnO_{3+d}$. A study of Mizusaki *et al.* (21) indicated that the maximum value of $d$ decreases with increasing $x$ to zero at $x = 0.4$ for $La_{1-x}Sr_xMnO_{3+d}$. Tamura and Yamamoto (22) studied the oxygen deficiency $y$ and the lattice constants of $La_{0.8}Ca_{0.2}MnO_{3-y}$, and Tanaka *et al.* (23) measured electrical and thermoelectric properties of these materials. The magnetoresistance of $La_{0.67}Ba_{0.33}MnO_z$ was studied by Ju *et al.* (24) as a function of oxygen stochiometry for $z = 2.99$ to 2.80. We have established synthesis conditions for obtaining stoichiometric $La_{1-x}Ba_xMnO_3$ materials and studied their properties (25).

Most of the recent work on the CMR properties of substituted $LaMnO_{3+d}$ materials was done on samples synthesized in air followed by slow cooling (4, 26–37). Using TGA measurements we have recently shown that oxygen nonstoichiometry for slowly cooled or high-oxygen-pressure annealed $La_{0.74}Ca_{0.26}MnO_{3+d}$ can be quite large, $0 \leq d \leq 0.066$ (8). By correlating resistive and magnetic properties of $d$, we have shown that, for example, $T_c$ can be changed by as much as 60 K within this range of nonstoichiometry. Thus, when comparing various $La_{1-x}A_xMnO_3$ materials whose properties are complex and very sensitive to hole concentration, $h = x + 2d$, it is of critical importance to report the proper chemical stoichiometry. For the investigation of intrinsic CMR properties it is especially important to establish synthesis conditions for obtaining stoichiometric materials with various substitution levels $x$.

We report here a study of the oxygen content and structural properties for a series of $La_{1-x}Ca_xMnO_3$ samples with $x = 0.00$–$0.38$. The magnetoresistive properties of these samples will be published separately (38). Using high sensitivity thermogravimetric measurements we have determined the oxygen content, $3 + d$, for samples synthesized under several oxygen pressures and temperatures to 1400°C. The most favorable synthesis conditions for obtaining stoichiometric samples have been determined and are listed in Fig. 6. The structures of the samples and unit cell volumes were measured at room temperature, confirming increased hole doping with increased defect concentration. Results show that, in addition to the commonly observed orthorhombic *Pbnm* O′ and O* structures, the rhombohedral $R\bar{3}c$ ($R$) (39, 40) structure is stabilized at high effective oxygen contents for $x \leq 0.14$.

## SAMPLE PREPARATION AND EXPERIMENTAL DETAILS

Polycrystalline samples of $La_{1-x}Ca_xMnO_3$ were synthesized from stoichiometric mixtures of $La_2O_3$ (Aesar, 99.999%, prefired in Ar at 700°C), $MnO_2$ (Aesar, 99.999%, stoichiometry was checked using thermogravimetry), and $CaCO_3$ (Aesar, 99.999%). The $x = 0.14$, 0.18, 0.22, 0.26, 0.30, 0.34, and 0.38 materials were processed using the standard ceramic method and fired in air several times at various temperatures up to 1400°C followed by fast cooling to room temperature. The ceramic method leads to low-density samples that are well suited for thermogravimetric measurements.

Samples with $x = 0$, 0.06, and 0.10 were synthesized using a wet-chemistry method by dissolving the oxides and carbonates in citric and nitric acids. Solutions were dried at 200–300°C and decomposed in air at 500–800°C. Firing was done in air at 1450°C followed by fast cooling to room temperature on a Cu-plate. This wet-chemistry synthesis method leads to dense samples with homogenous mixing of metal ions. Because these dense samples showed much slower oxygen kinetics during initial tests, the materials were ground to fine powders before annealings at high oxygen pressures and subsequent TGA measurements.

Parts of large (10 g) samples were annealed at 800°C for two days in pure oxygen, at 12 and 140 atm pressure. The crystal structures were studied by powder X-ray diffraction using a Rigaku powder diffractometer with Cu$K\alpha$ radiation. The effective oxygen contents were determined by TGA measurements using a Cahn TG171 system with slow heating (1–2 deg/min) and cooling (0.6 deg/min) rates. Pure reaction gases of 100, 20, 1, and 0.01% oxygen in argon (99.999%), $H_2$ (99.999%), and Ar (99.999%) as well as the gas mixtures of $O_2$/Ar and $H_2$/Ar were flowed at 100 cc/min using an MKS gas flow controller. About 1.2 grams of powders (for $x = 0$–$0.10$) or small chunks (for $x =$ 0.14–0.38) were heated in Alumina crucibles suspended on

Pt or Mo (for $H_2$/Ar reductions) wires. The weights of the samples were measured to 1 μg. Empty crucible TGA runs in pure gases and gas mixtures were used for calibration and buoyancy corrections. No sublimation of Ca or Mn was observed visually and the observation of constant weights of samples at 1400°C for 2 h confirmed that such problems were not present. Reproducibility of the data was checked several times using identical TGA conditions for samples with the same $x$. These measurements imply that the error bars for oxygen content are smaller than $\pm 0.002$, with the largest uncertainty arising from the morphology of the samples, which affects the kinetics of oxygen equilibrium.

## THERMOGRAVIMETRIC MEASUREMENTS

### 1. $LaMnO_{3+d}$

Data from a typical sequence of TGA measurements are shown in Fig. 1 for a $LaMnO_{3+d}$ sample annealed at 12 atm $O_2$ at 800°C. The material was slowly heated to 1400°C and cooled to 400°C, first in a 5% $O_2$/Ar gas mixture ($\log P(O_2) = -1.3$), and then, in 0.1% $O_2$/Ar ($\log P(O_2) = -3$). The absolute oxygen content, to which the TGA measurements were normalized, was determined by reduction in 50% $H_2$/Ar at 1100°C (see Fig. 1, insert). Based on X-ray diffraction of the reduced material that revealed two phases, $La_2O_3$ and MnO, the observed weight loss in hydrogen, $\Delta d$ corresponds to $0.582 \pm 0.002$, $0558 \pm 0.002$, and $0.500 \pm 0.002$ for samples obtained after slow cooling in 1 and 0.1% $O_2$/Ar, and fast cooling in Ar($\log P(O_2) \sim -5$), respectively.

Consequently, the initial oxygen content for the sample annealed at 12 atm is $3.178 \pm 0.002$. Since there is no excess oxygen defect site in the crystal structure, but vacancies form in approximately equal amounts on both metal sites, La and Mn, we can estimate the vacancy concentration of this material as $v \sim 0.056$. The oxygen content decreases during heating in 5% $O_2$/Ar and is $3.007 \pm 0.002$ ($v \sim 0.002$) at 1400°C. On cooling to 600°C, the oxygen content increases to $3.105 \pm 0.002$ ($v \sim 0.034$). Since the data on slow heating and cooling in 5% $O_2$ is almost fully reproducible in the temperature range 1150–1400°C ($\Delta d < 0.04$), the sample is close to thermal equilibrium at these temperatures.

On a subsequent heating in 0.1% $O_2$/Ar the oxygen content decreases to $3.000 \pm 0.002$ around 1300°C and remains virtually unchanged to 1400°C. On cooling, the oxygen content increases to $3.058 \pm 0.002$ ($v \sim 0.019$) at 600°C. The data on heating and cooling in 0.1% $O_2$ is again almost fully reproducible in a somewhat narrower temperature range, 1200–1400°C. Much slower heating and cooling rates or long holding times would be required to achieve well-equilibrated samples at lower temperatures than 1200°C (13–16). No significant changes in oxygen content were seen below 600°C during either heating or cooling in 0.1 and 5% $O_2$.

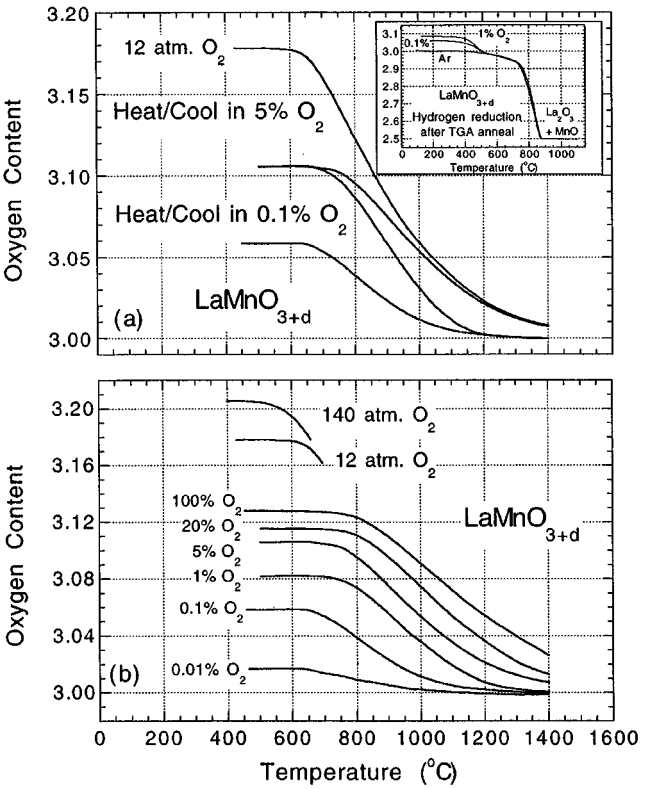


**FIG. 1.** Thermogravimetric analysis data for $LaMnO_{3+d}$, (a) sample annealed at 12 atm $O_2$ at 800°C, heated and cooled in 5% and 0.1% $O_2$; (b) cooling curves in 100, 20, 5, 1, and 0.01% $O_2$, and initial parts of heating curves for samples annealed in 12 and 140 atm $O_2$. (insert) Reduction in 50% $H_2$/Ar for samples obtained after slow cooling in 1 and 0.1% $O_2$, and fast cooling in Ar.

Similar TGA measurements were performed at several other partial pressures of oxygen. Figure 2 shows data obtained on cooling in 100, 20, 5, 1, 0.1, and 0.01% $O_2$/Ar as well as initial parts of heating curves for samples annealed in 12 and 140 atm $O_2$. Oxygen contents significantly above 3.000 have been achieved by prolonged annealings at 12 and 140 atm $O_2$ at 800°C and during slow cooling in oxygen or air. The maximum value of $d = 0.205$ is significantly lower than the value reported recently by Alonso *et al.* (17) for samples annealed at 200 atm $O_2$, but agrees with findings of Shimoyama *et al.* (41). The morphology and thermal history of samples may be the reason for the differences, since our samples were synthesized at 1400°C before annealing at 800°C while Alonso *et al.* (17) obtained their samples by direct synthesis using high oxygen pressure at 700–1000°C.

The values of oxygen content measured under various conditions are listed in Table 1. Clearly it is not possible to attain the stoichiometric composition in air below 1400°C. Such samples can be made only at reduced oxygen pressures and high temperatures, for example 0.1% $O_2$ at 1400°C.

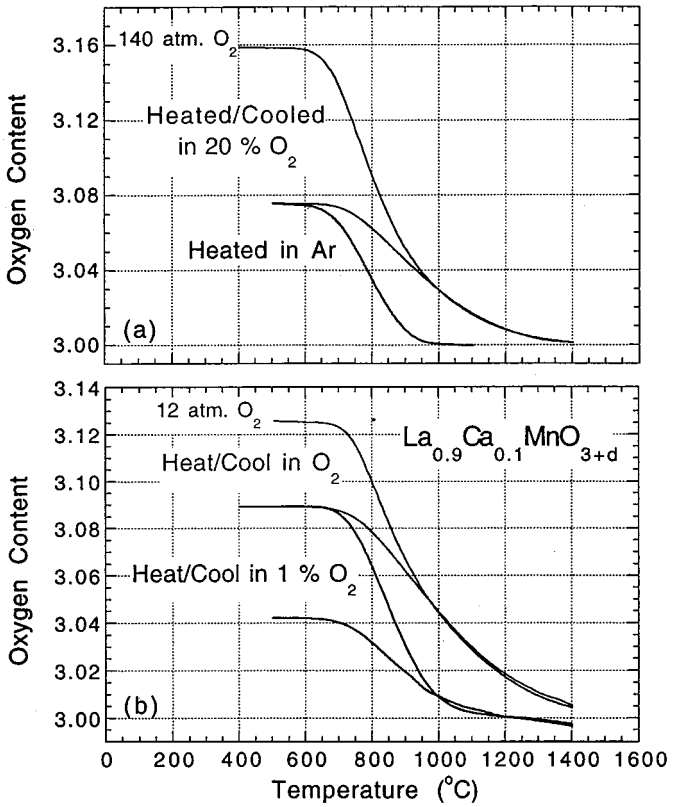


**FIG. 2.** Thermogravimetric analysis data for $La_{0.9}Ca_{0.1}MnO_{3+d}$ sample using (a) heating and cooling in 20% $O_2$ and heating in pure Ar. The starting material was annealed at 140 atm $O_2$; (b) heating and cooling in 100 and 1% $O_2$. The starting material was annealed at 12 atm $O_2$.

During TGA runs at oxygen contents larger than 0.1% $O_2$, samples appear to be in thermal equilibrium for temperatures of 1200–1400°C. Our data obtained at constant partial pressures of oxygen for slowly changing temperatures is in good agreement with previous results obtained as a function of the partial pressure of oxygen at fixed temperatures (14, 15). Our data show, nevertheless, consistently slightly smaller values of $d$ when compared with the data of Shimoyama *et al.* (41) at 1200°C indicating that a small temperature offset may have existed between these two measurements.

### *II. $La_{1-x}Ca_xMnO_{3+d}$*

TGA measurements were performed in Ar and in 100, 20, and 1% $O_2$, for $La_{1-x}Ca_xMnO_{3+d}$ ($x = 0.06$–$0.38$) samples annealed in 12 and 140 atm $O_2$ at 800°C. Figures 2–4 show a typical sequence of measurements for $x = 0.10$, 0.18, and 0.30. The normalization of the measurements was done by assuming that an absolute oxygen content of 3.000 is obtained at the center of an extended weight plateau in Ar at 1000–1110°C and in 1% $O_2$ at 1100–1300°C. The specific temperature for assignment of the nonstoichiometric compositions depends on the Ca substitution level, $x$, and was verified by a reduction in 50% $H_2$/Ar at 1100°C to $La_2O_3$ and a mixed oxide $Ca_{x/(1+x)}Mn_{1/(1+x)}O$ with an accuracy of $\pm 0.002$ (8).

Figure 2(a) shows the TGA data on heating and cooling in 20% $O_2$ ($\log P(O_2) = -0.7$) and on subsequent heating in Ar for the sample $x = 0.10$ annealed at 140 atm $O_2$. The starting oxygen content is $3.159 \pm 0.002$ ($v \sim 0.050$). The oxygen content decreases on heating to 3.000 around 1400°C and increases on cooling to $3.077 \pm 0.002$ ($v \sim 0.026$) at 650°C. The very good reproducibility of the data on heating and cooling in 20% $O_2$ at the temperature range 950–1400°C ($\Delta d < 0.002$), shows that the sample is near thermal equilibrium.

The fast kinetics of oxygen and metal ion observed in 20% $O_2$/Ar (artificial air) at these temperatures makes it simple to obtain samples with a designed oxygen content, $0 \leq d \leq 0.040$ (i.e., a vacancy concentration of $0 \leq v \leq 0.013$), by quenching in air from an appropriate temperature that can be read from Fig. 2(a). Also, the kinetics in Ar at this temperature is fast enough for samples to be in equilibrium when heated at 1 deg/min as confirmed by observation of constant sample weight at 1110°C for 10 h. The data indicate that a stoichiometric $x = 0.10$ sample can be obtained by quenching in air from ~1450°C or in Ar from 1050°C.

Figure 2(b) shows the TGA data in 100 and 1% $O_2$ for starting material annealed at 12 atm $O_2$. The normalization of the oxygen content to 3.000 was done at the center of an extended weight plateau near 1200°C in 1% $O_2$. The oxygen content can be read directly from Fig. 2(b) for the materials in thermal equilibrium at 950–1400°C in 100% $O_2$, and at 1000–1400°C in 1% $O_2$, as well as for the high pressure annealed and slowly cooled samples. To obtain stoichiometric sample in pure oxygen would require temperatures much higher than 1400°C. Quite large oxygen contents are produced during slow cooling in oxygen, air or 1% $O_2$, $d \sim 0.09$, 0.07, and 0.04, respectively. Conversely, small amounts of oxygen deficiency ($d < 0$) can be created in 1% $O_2$ and lower oxygen pressures at temperatures above 1250°C.

Figures 3 and 4 show that the value of $d$ decreases steadily with increasing $x$ for $La_{1-x}Ca_xMnO_{3+d}$ samples in thermal equilibrium at ~1000–1400°C, as well as for the high pressure annealed and slowly cooled samples. Consequently, the temperatures for obtaining stoichiometric samples in 20%, 1% or Ar decrease with increasing $x$. For $x \geq 0.34$, a stoichiometric sample can be made by slow cool in air or 1% $O_2$, and for $x \geq 0.38$ also in pure oxygen. The most favorable synthesis conditions for obtaining stoichiometric samples can be read from these TGA curves

**TABLE 1**

**The Oxygen Content, Structural Phases (the Orthorhombic *Pbnm* ($c/a < \sqrt{2}$)–O′, ($a \sim b \sim c/\sqrt{2}$)–O*, the Rhombohedral $R\bar{3}c$-*R*), Lattice Parameters and Angles, and Volume per Formula Unit for $La_{1-x}Ca_xMnO_{3+d}$ Samples, Annealed at 12 and 140 atm $O_2$ at 800°C, Slowly Cooled on TGA, and Fast Cooled in Ar or Air**

| Substitution synthesis | Oxygen content Structural phase | | *a* (Å) | *b* (Å) | *c* (Å) | Angle (°) | Volume (Å$^3$)/ formula unit |
|---|---|---|---|---|---|---|---|
| $x = 0.0$ | (± 0.002) | | | | | | |
| Ar (0.001%) | 3.000 | O′ | 5.5338(4) | 5.7373(4) | 7.6936(6) | | 61.066 |
| 0.01% | 3.017 | O′ | 5.5355(5) | 5.7096(5) | 7.7007(7) | | 60.847 |
| 0.1% | 3.057 | O* | 5.5303(8) | 5.5569(8) | 7.7718(11) | | 59.709 |
| 1% | 3.082 | O* | 5.5068(5) | 5.5401(5) | 7.7906(8) | | 59.418 |
| 5% | 3.106 | O* | 5.4933(4) | 5.5368(4) | 7.7680(6) | | 59.154 |
| 20% | 3.116 | *R* | 5.4893 (9) | | | 60.426(5) | 59.045 |
| 100% | 3.128 | *R* | 5.4713(3) | | | 60.672(2) | 58.784 |
| 12 atm | 3.178 | *R* | 5.4625(3) | | | 60.563(2) | 58.362 |
| 140 atm | 3.205 | *R* | 5.4565(4) | | | 60.536(2) | 58.133 |
| $x = 0.06$ | | | | | | | |
| Ar (0.001%) | 3.000 | O′ | 5.5301(4) | 5.6622(5) | 7.7046(6) | | 60.313 |
| 1% | 3.060 | O* | 5.5067(5) | 5.5297(6) | 7.7832(8) | | 59.251 |
| 20% | 3.095 | O* | 5.4856(5) | 5.5263(5) | 7.7640(8) | | 58.842 |
| 100% | 3.110 | *R* | 5.4759(7) | | | 60.396(4) | 58.571 |
| 12 atm | 3.140 | *R* | 5.4556(3) | | | 60.609(1) | 58.200 |
| 140 atm | 3.172 | *R* | 5.4505(2) | | | 60.568(1) | 57.982 |
| $x = 0.10$ | | | | | | | |
| Air 1450°C | 3.000 | O′ | 5.5258(5) | 5.6034(5) | 7.7181(7) | | 59.745 |
| 1% | 3.042 | O* | 5.5009(5) | 5.5221(7) | 7.7760(8) | | 59.053 |
| 20% | 3.077 | O* | 5.4827(4) | 5.5187(4) | 7.7568(6) | | 58.674 |
| 100% | 3.089 | O* | 5.4764(4) | 5.5163(4) | 7.7476(6) | | 58.513 |
| 12 atm | 3.126 | *R* | 5.4510(2) | | | 60.591(1) | 58.027 |
| 140 atm | 3.159 | *R* | 5.4465(2) | | | 60.580(1) | 57.871 |
| $x = 0.14$ | | | | | | | |
| air 1425°C | 3.000 | O′ | 5.5206(8) | 5.5701(7) | 7.7308(10) | | 59.432 |
| air 1425°C | 3.000 | O* | 5.5075(8) | 5.5327(9) | 7.7692(11) | | 59.183 |
| 1% | 3.026 | O* | 5.4999(6) | 5.5162(9) | 7.7731(10) | | 58.956 |
| 20% | 3.053 | O* | 5.4855(4) | 5.5147(4) | 7.7590(7) | | 58.679 |
| 100% | 3.074 | O* | 5.4747(4) | 5.5097(5) | 7.7423(7) | | 58.384 |
| 12 atm | 3.102 | O* | 5.4623(4) | 5.5040(4) | 7.7266(7) | | 58.074 |
| 140 atm | 3.130 | *R* | 5.4443(5) | | | 60.534(2) | 57.743 |
| $x = 0.18$ | | | | | | | |
| air 1400°C | 3.000 | O* | 5.5034(2) | 5.5077(3) | 7.7651(12) | | 58.841 |
| 1% | 3.014 | O* | 5.4923(5) | 5.5104(7) | 7.7629(8) | | 58.736 |
| 20% | 3.037 | O* | 5.4817(4) | 5.5084(5) | 7.7500(6) | | 58.504 |
| 100% | 3.054 | O* | 5.4722(4) | 5.5027(4) | 7.7383(6) | | 58.255 |
| 12 atm | 3.090 | O* | 5.4609(4) | 5.4973(4) | 7.7193(6) | | 57.934 |
| 140 atm | 3.105 | O* | 5.4531(5) | 5.4932(6) | 7.7121(9) | | 57.753 |
| $x = 0.22$ | | | | | | | |
| air 1350°C | 3.000 | O* | 5.4833(6) | 5.5042(8) | 7.7491(8) | | 58.468 |
| 1% | 3.004 | O* | 5.4846(5) | 5.5037(7) | 7.7525(8) | | 58.503 |
| 20% | 3.021 | O* | 5.4746(4) | 5.4992(5) | 7.7389(7) | | 58.247 |
| 100% | 3.035 | O* | 5.4699(4) | 5.4971(5) | 7.7339(7) | | 58.137 |
| 12 atm | 3.067 | O* | 5.4582(4) | 5.4905(4) | 7.7154(6) | | 57.804 |
| 140 atm | 3.088 | O* | 5.4502(4) | 5.4877(4) | 7.7028(6) | | 57.596 |
| $x = 0.26$ | | | | | | | |
| air 1300°C | 3.000 | O* | 5.4745(10) | 5.4929(9) | 7.7360(15) | | 58.157 |
| 1% | 3.003 | O* | 5.4774(9) | 5.4923(9) | 7.7379(19) | | 58.196 |
| 20% | 3.008 | O* | 5.4732(4) | 5.4881(4) | 7.7460(9) | | 58.168 |
| 100% | 3.017 | O* | 5.4723(11) | 5.4887(9) | 7.7314(18) | | 58.055 |
| 12 atm | 3.043 | O* | 5.4644(5) | 5.4811(6) | 7.7095(15) | | 57.727 |
| 140 atm | 3.066 | O* | 5.4528(14) | 5.4666(9) | 7.6729(18) | | 57.179 |

**TABLE 1**—*Continued*

| Substitution synthesis | Oxygen content Structural phase | | *a* (Å) | *b* (Å) | *c* (Å) | Angle (°) | Volume (Å$^3$)/ formula unit |
|---|---|---|---|---|---|---|---|
| $x = 0.30$ | | | | | | | |
| air 1200°C | 3.000 | O* | 5.4624(4) | 5.4806(4) | 7.7208(6) | | 57.784 |
| 12 atm | 3.027 | O* | 5.4479(4) | 5.4755(5) | 7.6967(7) | | 57.399 |
| 140 atm | 3.045 | O* | 5.4412(5) | 5.4601(6) | 7.6830(7) | | 57.064 |
| $x = 0.34$ | | | | | | | |
| air slow cool | 3.000 | O* | 5.4544(5) | 5.4758(7) | 7.7052(8) | | 57.533 |
| 140 atm | 3.026 | O* | 5.4527(6) | 5.4724(8) | 7.7011(8) | | 57.450 |
| $x = 0.38$ | | | | | | | |
| air slow cool | 3.000 | O* | 5.4422(5) | 5.4610(6) | 7.6865(8) | | 57.111 |
| 140 atm | 3.011 | O* | 5.4402(5) | 5.4617(6) | 7.6806(8) | | 57.053 |

and are also listed in Fig. 6. The oxygen contents for the studied samples, annealed at 12 and 140 atm $O_2$ at 800°C, slowly cooled on TGA in 1, 20, and 100% $O_2$, and fast cooled in Ar or air, are given in Table 1.

## OXYGEN CONTENT AND THE HOLE DOPING

Compilation of the data for measured oxygen contents that were obtained for slow-cooled samples on TGA

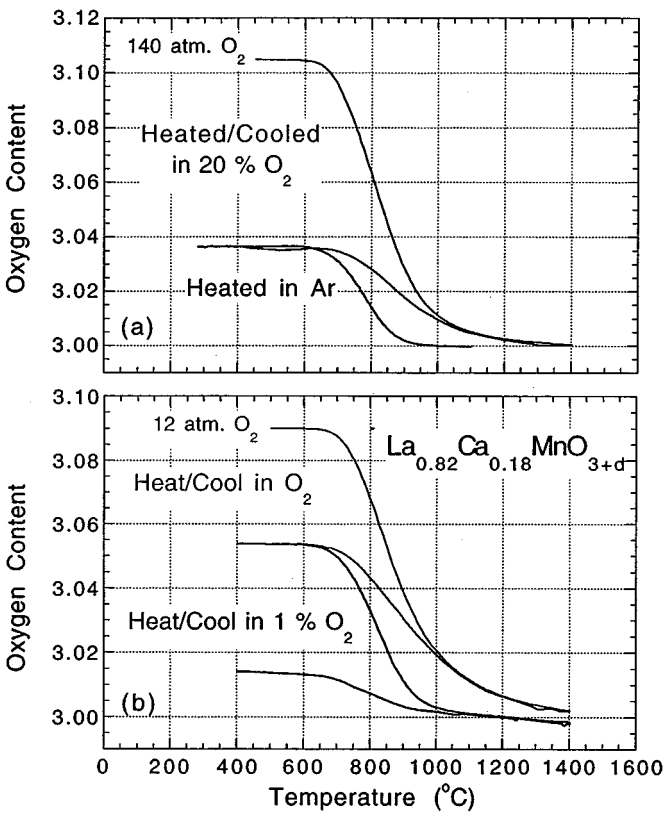


**FIG. 3.** Thermogravimetric analysis data for $La_{0.82}Ca_{0.18}MnO_{3+d}$ sample using (a) heating and cooling in 20% $O_2$ and heating in pure Ar. The starting material was annealed at 140 atm $O_2$; (b) heating and cooling in 100 and 1% $O_2$. The starting material was annealed at 12 atm $O_2$.

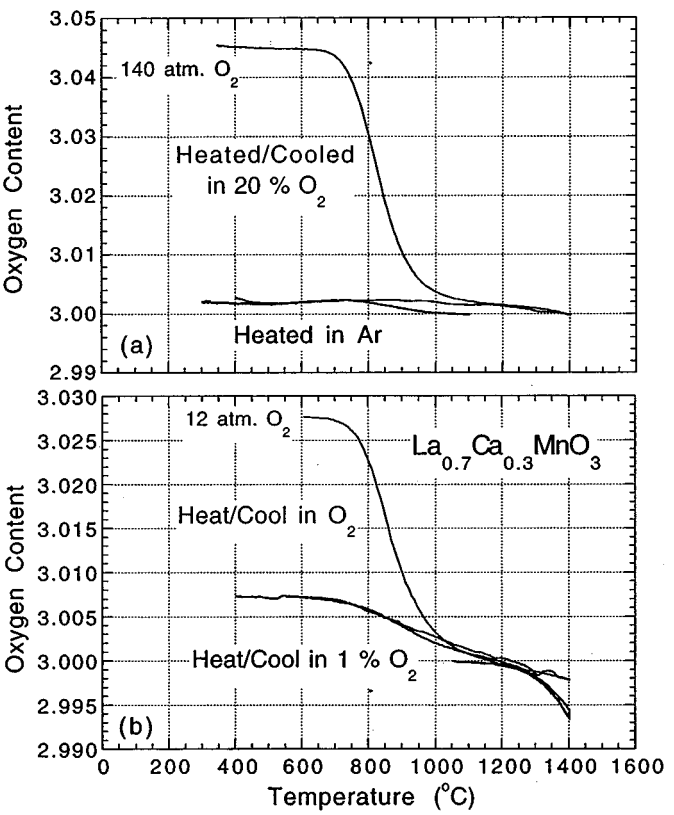


**FIG. 4.** Thermogravimetric analysis data for $La_{0.7}Ca_{0.3}MnO_{3+d}$ sample using (a) heating and cooling in 20% $O_2$ and heating in pure Ar. The starting material was annealed at 140 atm $O_2$; (b) heating and cooling in 100 and 1% $O_2$. The starting material was annealed at 12 atm $O_2$.

apparatus and materials annealed at high-oxygen-pressure is shown in Fig. 5. Clearly the oxygen content that can be attained by these processes decreases with increasing $x$ from very large values at $x = 0$, to near stoichiometric compositions at $x = 0.38$. We have observed previously a similar decrease of oxygen nonstoichiometry for $La_{1-x}Ba_xMnO_3$ materials with $0.10 \leq x \leq 0.24$ (25). Our results for the maximum oxygen nonstoichiometry of $La_{1-x}Ca_xMnO_{3+d}$ are quite comparable to values obtained for $La_{1-x}Sr_xMnO_{3+d}$ samples during very long annealings in oxygen at low temperatures, $\sim 600^\circ$C (14, 15).

Slow-cooling on the TGA done in 20% $O_2$ produces samples that are similar to those from a typical furnace-cool in air used during synthesis of CMR materials. Our results show that these slow-cooling processes can introduce substantial oxygen nonstoichiometry for $x \leq 0.26$ that may affect CMR properties in a noticeable way (8). The large defect concentrations may cause significant increases of the average Mn oxidation state and also introduce local structural distortions and electronic nonhomogeneity that would affect structural, transport and magnetic properties. The data shown in Figs. 2–5 can be used to estimate the amount of hole doping for materials obtained previously by various synthesis methods. Assuming charge neutrality and a uniform vacancy distribution on the cation sites, the extra hole doping by defects is $\Delta h = 2d$. Figure 6 summarizes the determined hole doping, $h = x + 2d$, for $La_{1-x}Ca_xMnO_{3+d}$ samples obtained by high-oxygen-pressure annealings and slow cooling in 1, 20, and 100% $O_2$. It is surprising that annealings at a specific temperature and oxygen pressure lead to approximately constant hole doping (Mn oxidation state) over an extended range of substitution $x$. As a consequence, using identical synthesis conditions for a series of samples will result in materials with similar hole doping and variation of properties that would be caused mostly by varying vacancy content on the metal sites.

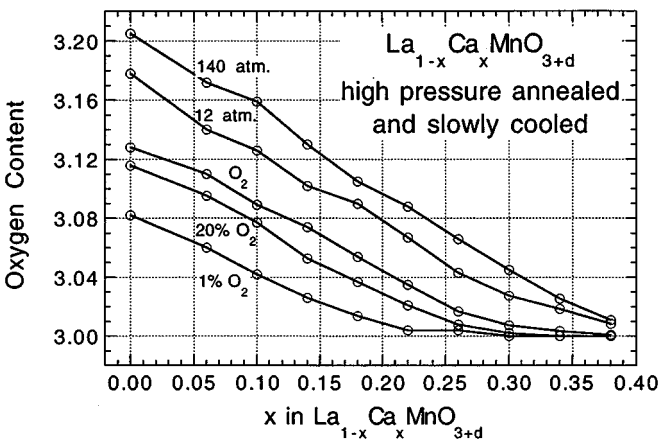


**FIG. 5.** Oxygen content for slow-cooled samples on the TGA apparatus and materials annealed at high-oxygen-pressure for $La_{1-x}Ca_xMnO_{3+d}$.

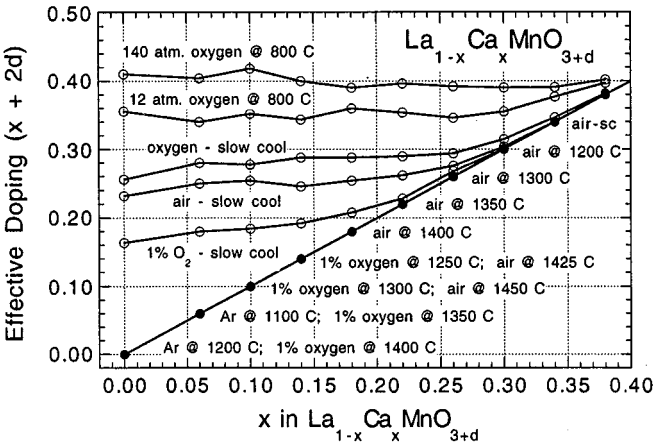


**FIG. 6.** Effective hole doping, $h = x + 2d$, for $La_{1-x}Ca_xMnO_{3+d}$ samples obtained by high-oxygen-pressure annealings and slow cooling on the TGA apparatus. The most favorable synthesis conditions for obtaining stoichiometric samples are listed for various $x$.

Figure 6 also lists the most favorable synthesis conditions for obtaining stoichiometric samples, $h = x$ ($d = 0$). For a specific oxygen pressure, for example during synthesis in air, a rather wide range of temperatures near the optimum (at least $\pm 50^\circ$C) can usually be used without introduction of noticeable nonstoichiometry. It is important to recognize that conditions for obtaining stoichiometric samples apply equally well to bulk powders and single crystals. The synthesis of powders is usually done by repeated grinding and firing at 1200–1400°C, and, thus, can easily be tuned to produce stoichiometric material without further annealing. Crystal growth is done at temperatures of 1600°C and higher, i.e., under conditions where material usually forms considerable oxygen vacancy concentration. Further annealing is then required to produce stoichiometric material. However, if the conditions of the anneal are not chosen properly, the annealed crystals may contain cation vacancies. A review of the synthesis conditions used to date for bulk powders and single crystals indicates that several studies reported in the literature were done on significantly nonstoichiometric materials.

## STRUCTURAL PROPERTIES

All samples prepared at high oxygen pressure and on the TGA apparatus were characterized by powder X-ray diffraction at room temperature. Data were collected from 20–70° in $2\theta$ with a step size of 0.04° and a counting time of 2.5 s per step. The diffraction patterns could be indexed based on an orthorhombic unit cell with the space group *Pbnm* or rhombohedral unit cell with the space group $R\bar{3}c$. Figure 7 shows typical diffraction patterns for $x = 0.10$ corresponding to three distorted structural phases of the cubic perovskite structure that can be clearly identified as

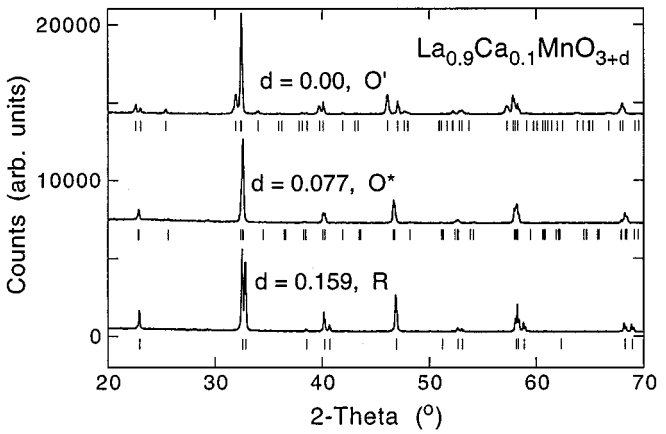


**FIG. 7.** X-ray diffraction patterns for $La_{0.9}Ca_{0.1}MnO_{3+d}$ samples with $d \sim 0.000$ (orthorhombic *Pbnm* structure O′ with $c/a < \sqrt{2}$), $d = 0.077 \pm 0.002$ (orthorhombic *Pbnm* structure O* with $a \sim b \sim c/\sqrt{2}$, and $d = 3.159 \pm 0.002$ (rhombohedral $R\bar{3}c$).

a function of the oxygen content. For stoichiometric material, the orthorhombic *Pbnm* structure (O′) characrterized by large coherent orbital ordering of the Jahn–Teller type and $c/a < \sqrt{2}$ is observed. The sample with oxygen content $3 + d = 3.077 \pm 0.002$ is orthorhombic (O*) with the same *Pbnm* structure but characterized by a considerably smaller coherent Jahn–Teller orbital ordering and $a \sim b \sim c/\sqrt{2}$. The sample with the largest oxygen content $3 + d = 3.159 \pm 0.002$ is rhombohedral with no coherent Jahn–Teller orbital ordering present.

Figure 8 shows the observed structures as a function of Ca substitution and effective oxygen content for all samples studied. Consistent with previous results, only the orthorhombic phases O′ and O* are present at room temperature as a function of $x$ for stoichiometric samples. The O′/O* phase boundary appears near $x = 0.14$, i.e., at a composition higher than is usually reported in the literature (27). The reason for the difference probably arises from comparing the behavior of compositions that are inaccurately assumed to have the same doping level. Because a variety of synthesis conditions have been employed to date, for example, annealing in air or oxygen in 1200°C followed by furnace cooling, the effective hole doping may be considerably larger than assumed for samples in the literature. Since, as Fig. 8 shows, increased hole concentration moves the O′ to O* transition to smaller $x$, nonstoichiometric samples will have the O* structure for $x$ smaller than the stoichiometric samples. For example, this effect can be clearly observed for the $x = 0$ sample. With increasing $d$ the structure transforms from O′ to O* near $d = 0.04$ and from O* to $R$, a structure that is not present for the stoichiometric samples, at $d = 0.11$. The effective oxygen contents at these transitions for our samples are in agreement with most of the previous studies (17, 39, 40). Our data show in addition that a similar sequence of structural transitions with increasing $d$ can be observed for $x = 0$–$0.14$ samples. Obviously, the hole doping is not the only parameter that controls the structure. The most important parameters are the relative sizes of the $A$ and $B$ ions, which are controlled by the hole doping (the $B$ site), and the average size and variance of sizes of the ions substituted on the $A$ site. In addition, vacancies on the $A$ and $B$ sites can produce local atom displacements that may affect the long-range structure.

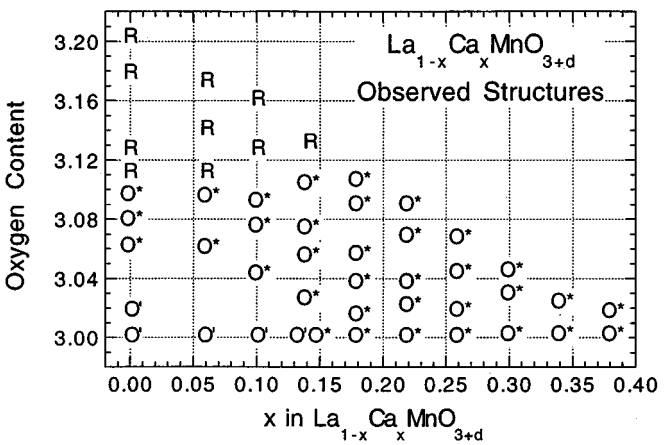


**FIG. 8.** Observed structural phases (orthorhombic *Pbnm* with $c/a < \sqrt{2}$–O′, orthorhombic *Pbnm* with $a \sim b \sim \sqrt{2}$–O*, and rhombohedral $R\bar{3}c$-$R$) as a function of oxygen content $d$ and composition $x$ for $La_{1-x}Ca_xMnO_{3+d}$.

The X-ray diffraction data were analyzed using the Rietveld technique with the GSAS program (42). For all patterns, background, peak width, and zero shift were refined along with the lattice parameters, atomic positions, and isotropic thermal parameters. The thermal parameters for oxygen were kept fixed at 0.8 Å$^2$. Refinements were carried out in space groups $R\bar{3}c$ and *Pbnm*, depending on $x$ and $d$. No impurity phases were found in any of the patterns. Refined lattice parameters and unit cell volumes per formula unit are given in Table 1 for all the samples. A clear decrease of the unit cell volume is observed with increasing $x$ for stoichiometric samples and with increasing $d$ for samples with fixed $x$. The dependence of the unit cell volume on the hole doping, $h = x + 2d$, is shown in Fig. 9. The unit cell volume decreases steadily with hole doping irrespective of the source of doping, Ca substitution for La or oxygen content (vacancy formation on the cation sites). A slightly faster decrease of the unit cell volume is observed for an equivalent amount of doping by Ca substitution for La than for vacancy formation on cation sites. The decrease of the unit cell volume with increasing $d$ confirms that the additional holes are doped by defects at both metal sites for all studied $x$.

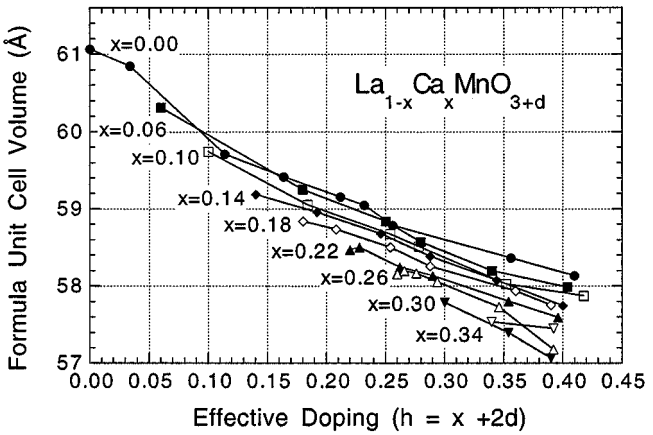


**FIG. 9.** Unit cell volume versus the hole doping $h = x + 2d$ for $La_{1-x}Ca_xMnO_{3+d}$.

## CONCLUSION

By annealing at atmospheric and high oxygen pressures between 700 and 1200°C a substantial amount of vacancies can be generated for $La_{1-x}Ca_xMnO_3$ samples with $x \leq 0.30$. Thermogravimetric analysis measurements provide an accurate measurement of the oxygen content and allow the determination of synthesis conditions for preparation of stoichiometric samples. Each composition requires unique synthesis conditions since annealing under identical temperature and oxygen pressure leads to approximately constant hole doping over an extended range of Ca substitution, $x$, and to materials with variable properties resulting mostly from the varying vacancy contents on the cation sites. The structural properties are governed by the relative sizes of the $A$- and $B$-site ions which are controlled by the hole doping (the $B$-site size), the sizes of ions substituted on the $A$ site as well as concentration of vacancies on $A$ and $B$ sites. A sequence of observed structural transitions, O′ to O* to $R$, and a decrease of the unit cell volume with increasing $d$ confirm that the additional holes are doped uniformly by cation vacancy defects similar to the Ca substitution, $x$.

## ACKNOWLEDGMENTS

This work at NIU was supported by the ARPA/ONR and at ANL by US DOE (W-31-109-ENG-38).

## REFERENCES

1. J. P. P. Huijsmans, E. J. Siewers, F. H. van Heuveln, and J. P. de Jong, *in* "Proc. Second International Symposium on Solid Oxide Fuel Cells, Athens, 1991" (F. Grosz, P. Zegers, S. C. Singhal, and O. Yamamoto, Eds.), pp. 113–118.
2. R. J. H. Voorhove J. P. Remeika, L. E. Trimble, A. S. Cooper, F. J. Disalvo, and P. K. Gallagher, *J. Solid State Chem* **14,** 395 (1975).
3. R. M. Kusters, J. Singelton, D. A. Keen, R. McGreevy, and W. Hayes, *Physica B* **155,** 362 (1989).
4. A. Urushibara, Y. Moritomo, T. Arima, A. Asamitsu, G. Kido, and Y. Tokura, *Phys. Rev. B* **51,** 14103 (1995).
5. H. Y. Hwang, S.-W. Cheong, P. G. Radaelli, M. Marezio, and B. Batlogg, *Phys. Rev. Lett.* **75,** 914 (1995).
6. L. M. Rodriguez-Martinez and J. P. Attfield, *Phys. Rev. B* **54,** R15622 (1996).
7. C. Ritter, M. R. Ibarra, J. M. De Teresa, P. A. Algarabel, C. Marquina, J. Blasco, J. Garcia, S. Oseroff, and S.-W. Cheong, *Phys. Rev. B* **56,** 8902 (1997).
8. B. Dabrowski, P. W. Klamut, Z. Bukowski, R. Dybzinski, and J. E. Siewenie, unpublished manuscript.
9. K. Kamata, T. Nakajima, T. Hayashi, and T. Nakamura, *Mat. Res. Bull.* **13,** 49 (1978).
10. T. Nakamura, G. Petzlow, and L. J. Gauckler, *Mater. Res. Bull.* **14,** 649 (1979).
11. M. L. Borlera and F. Abbattista, *J. Less-Common Mat.* **92,** 55 (1983).
12. J. A. M. Van Roosmalen, E. H. P. Cordfunke, R. B. Helmholdt, and H. W. Zandbergen, *J. Solid State Chem.* **110,** 100 (1994).
13. J. A. M. Van Roosmalen and E. H. P. Cordfunke, *J. Solid State Chem.* **110,** 106 (1994).
14. J. A. M. Van Roosmalen and E. H. P. Cordfunke, *J. Solid State Chem.* **110,** 109 (1994).
15. J. A. M. Van Roosmalen and E. H. P. Cordfunke, *J. Solid State Chem.* **110,** 113 (1994).
16. J. Toepfer and J. B. Goodenough, *Chem. Mater.* **9,** 1467 (1997).
17. J. A. Alonso, M. J. Martinez-Lope, and M. T. Casais, *Eur. J. Solid State Inorg. Chem.* **33,** 331 (1996).
18. J. A. Alonso, M. J. Martinez-Lope, M. T. Casais, and A. Munoz, *Solid State Comm.* **102,** 7 (1997).
19. S. de Brion, F. Ciorcas, G. Chouteau, P. Lajay, P. Radaelli, and C. Chaillout, *Phys. Rev. B* **59,** 1304 (1999).
20. W. H. McCarroll, K. V. Ramanujachary, M. Greenblat, and F. Cosandey, *J. Solid State Chem.* **136,** 322 (1998).
21. J. Mizusaki, H. Tagawa, K. Naraya, and T. Sasamoto, *Solid State Ionics* **49,** 111 (1991).
22. S. Tamura and A. Yamamoto, *J. Mater. Sci. Lett.* **15,** 2120 (1980).
23. J. Tanaka, M. Umehara, S. Tamura, M. Tsukioka, and S. Ehara, *J. Phys. Soc. Jpn* **51,** 1236 (1982).
24. H. L. Ju, J. Gopalakrishnan, J. L. Peng, Qi Li, G. C. Xiong, T. Venkatesan, and R. L. Greene, *Phys. Rev. B* **51,** 6143 (1995).
25. B. Dabrowski, K. Rogacki, X. Xiong, P. W. Klamut, R. Dybzinski, J. Shaffer, and J. D. Jorgensen, *Phys. Rev. B* **58,** 2716 (1998).
26. M. Hervieu, R. Mahesh, N. Rangavittal, and C. N. R. Rao, *Eur. J. Solid State Inorg. Chem.* **32,** 79 (1995).
27. P. Schiffer, A. P. Ramirez, W. Bao, and S.-W. Cheong, *Phys. Rev. Lett.* **75,** 3336 (1995).
28. H. Roder, J. Zhang, and A. R. Bishop, *Phys. Rev. Lett.* **76,** 1356 (1996).
29. T. A. Tyson, J. Mustre de Leon, S. D. Conradson, A. R. Bishop, J. J. Neumeier, H. Roder, and J. Zang, *Phys. Rev. B* **53,** 13985 (1996).
30. R. H. Heffner, L. P. Le, M. F. Hundley, J. J. Neumeier, G. M. Luke, K. Kojima, B. Nachumi, Y. J. Uemura, D. E. MacLaughlin, and S.-W. Cheong, *Phys. Rev. Lett.* **77,** 1869 (1996).
31. K. H. Kim, J. Y. Gu, H. S. Choi, G. W. Park, and T. W. Noh, *Phys. Rev. Let.* **77,** 1877 (1996).
32. J.-H. Park, C. T. Chen, S.-W. Cheong, W. Bao, G. Meigs, V. Chakarin, and Y. U. Idzerda, *Phys. Rev. Lett.* **76,** 4215 (1996).
33. C. H. Booth, F. Bridges, G. H. Kwei, J. M. Lawrence, A. L. Cornelius, and J. J. Neumeier, *Phys. Rev. Lett.* **80,** 853 (1998).
34. H. Y. Hwang, S.-W. Cheong, P. G. Radaelli, M. Marezio, and B. Batlogg, *Phys. Rev. Lett.* **75,** 914 (1995).
35. M. Itoh, K. Nishi, J. D. Yu, and Y. Inaguma, *Phys. Rev. B* **55,** 14408 (1997).

36. P. G. Radaelli, G. Iannone, M. Marezio, H. Y. Hwang, S.-W. Cheong, J. D. Jorgensen, and D. N. Argyriou, *Phys. Rev. B* **56,** 8265 (1997).
37. S. J. L. Billinge, R. G. DiFrancesco, G. H. Kwei, J. J. Neumeier, and J. D. Thompson, *Phys. Rev. Lett*. **77,** 715 (1996).
38. Z. Bukowski, B. Dabrowski, O. Chmaissem, P. W. Klamut, R. Dybzinski, J. E. Siewenie, and C. W. Kimball, unpublished manuscript.
39. J. A. M. Van Roosmalen, P. van Vlaanderen, E. H. P. Cordfunke, W. L. Ijdo, and D. J. W. Ijdo, *J. Solid State Chem.* **114,** 516 (1995).
40. J. F. Mitchell, D. N. Argyriou, C. D. Potter, D. G. Hinks, J. D. Jorgensen, and S. D. Bader, *Phys. Rev. B* **54,** 6172 (1996).
41. J. Shimoyama, J. Mizusaki, and K. Fueki, "Fall Meeting, Chem. Soc. Japan," 3Q06 (1986).
42. A. C. Larson and R. W. von Dreele "General Structure Analysis system," University of California, 1985–1990.